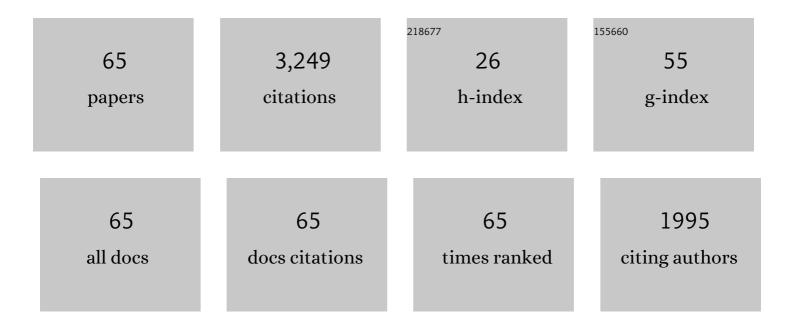
Shuliang Jiao

List of Publications by Year in descending order

Source: https://exaly.com/author-pdf/8947734/publications.pdf Version: 2024-02-01



SHULLANG LIAO

#	Article	lF	CITATIONS
1	Photoacoustic ophthalmoscopy for in vivo retinal imaging. Optics Express, 2010, 18, 3967.	3.4	251
2	Simultaneous acquisition of sectional and fundus ophthalmic images with spectral-domain optical coherence tomography. Optics Express, 2005, 13, 444.	3.4	245
3	Laser-scanning optical-resolution photoacoustic microscopy. Optics Letters, 2009, 34, 1771.	3.3	224
4	In Vivo Three-Dimensional High-Resolution Imaging of Rodent Retina with Spectral-Domain Optical Coherence Tomography. , 2007, 48, 1808.		210
5	Two-dimensional depth-resolved Mueller matrix of biological tissue measured with double-beam polarization-sensitive optical coherence tomography. Optics Letters, 2002, 27, 101.	3.3	202
6	Jones-matrix imaging of biological tissues with quadruple-channel optical coherence tomography. Journal of Biomedical Optics, 2002, 7, 350.	2.6	189
7	Optical-fiber-based Mueller optical coherence tomography. Optics Letters, 2003, 28, 1206.	3.3	151
8	Depth-resolved two-dimensional Stokes vectors of backscattered light and Mueller matrices of biological tissue measured with optical coherence tomography. Applied Optics, 2000, 39, 6318.	2.1	142
9	Determination of local polarization properties of biological samples in the presence of diattenuation by use of Mueller optical coherence tomography. Optics Letters, 2004, 29, 2402.	3.3	121
10	Simultaneous multimodal imaging with integrated photoacoustic microscopy and optical coherence tomography. Optics Letters, 2009, 34, 2961.	3.3	113
11	A combined method to quantify the retinal metabolic rate of oxygen using photoacoustic ophthalmoscopy and optical coherence tomography. Scientific Reports, 2014, 4, 6525.	3.3	106
12	Automatic retinal blood flow calculation using spectral domain optical coherence tomography. Optics Express, 2007, 15, 15193.	3.4	96
13	Integrating photoacoustic ophthalmoscopy with scanning laser ophthalmoscopy, optical coherence tomography, and fluorescein angiography for a multimodal retinal imaging platform. Journal of Biomedical Optics, 2012, 17, 061206.	2.6	89
14	Contrast mechanisms in polarization-sensitive Mueller-matrix optical coherence tomography and application in burn imaging. Applied Optics, 2003, 42, 5191.	2.1	75
15	Combined photoacoustic microscopy and optical coherence tomography can measure metabolic rate of oxygen. Biomedical Optics Express, 2011, 2, 1359.	2.9	74
16	Frequency-swept ultrasound-modulated optical tomography in biological tissue by use of parallel detection. Optics Letters, 2000, 25, 734.	3.3	70
17	In Situ Visualization of Tears on Contact Lens Using Ultra High Resolution Optical Coherence Tomography. Eye and Contact Lens, 2009, 35, 44-49.	1.6	59
18	Optical coherence tomography for whole eye segment imaging. Optics Express, 2012, 20, 6109.	3.4	51

SHULIANG JIAO

#	Article	IF	CITATIONS
19	Optical coherence photoacoustic microscopy for in vivo multimodal retinal imaging. Optics Letters, 2015, 40, 1370.	3.3	48
20	Optical coherence photoacoustic microscopy: accomplishing optical coherence tomography and photoacoustic microscopy with a single light source. Journal of Biomedical Optics, 2012, 17, 030502.	2.6	45
21	Fiber-based polarization-sensitive Mueller matrix optical coherence tomography with continuous source polarization modulation. Applied Optics, 2005, 44, 5463.	2.1	43
22	Simultaneous in vivo imaging of melanin and lipofuscin in the retina with photoacoustic ophthalmoscopy and autofluorescence imaging. Journal of Biomedical Optics, 2011, 16, 080504.	2.6	40
23	Dual channel dual focus optical coherence tomography for imaging accommodation of the eye. Optics Express, 2009, 17, 8947.	3.4	39
24	Dual-band spectral-domain optical coherence tomography for in vivo imaging the spectral contrasts of the retinal nerve fiber layer. Optics Express, 2011, 19, 19653.	3.4	38
25	Registration of high-density cross sectional images to the fundus image in spectral-domain ophthalmic optical coherence tomography. Optics Express, 2006, 14, 3368.	3.4	37
26	Retinal tumor imaging and volume quantification in mouse model using spectral-domain optical coherence tomography. Optics Express, 2009, 17, 4074.	3.4	36
27	Collecting back-reflected photons in photoacoustic microscopy. Optics Express, 2010, 18, 1278.	3.4	34
28	Dual band dual focus optical coherence tomography for imaging the whole eye segment. Biomedical Optics Express, 2015, 6, 2481.	2.9	27
29	In vivo burn imaging using Mueller optical coherence tomography. Optics Express, 2008, 16, 10279.	3.4	25
30	Simultaneous dual molecular contrasts provided by the absorbed photons in photoacoustic microscopy. Optics Letters, 2010, 35, 4018.	3.3	24
31	Near-infrared light photoacoustic ophthalmoscopy. Biomedical Optics Express, 2012, 3, 792.	2.9	24
32	Fundus Camera Guided Photoacoustic Ophthalmoscopy. Current Eye Research, 2013, 38, 1229-1234.	1.5	23
33	Simultaneous optical coherence tomography and autofluorescence microscopy with a single light source. Journal of Biomedical Optics, 2012, 17, 080502.	2.6	21
34	Multimodal photoacoustic ophthalmoscopy in mouse. Journal of Biophotonics, 2013, 6, 505-512.	2.3	21
35	Effect of Contact Lens on Optical Coherence Tomography Imaging of Rodent Retina. Current Eye Research, 2013, 38, 1235-1240.	1.5	20
36	Systematic study of high-frequency ultrasonic transducer design for laser-scanning photoacoustic ophthalmoscopy. Journal of Biomedical Optics, 2014, 19, 016015.	2.6	20

Shuliang Jiao

#	Article	IF	CITATIONS
37	Adaptive optics photoacoustic microscopy. Optics Express, 2010, 18, 21770.	3.4	18
38	Image chorioretinal vasculature in albino rats using photoacoustic ophthalmoscopy. Journal of Modern Optics, 2011, 58, 1997-2001.	1.3	17
39	Visible-light optical coherence tomography-based multimodal retinal imaging for improvement of fluorescent intensity quantification. Biomedical Optics Express, 2016, 7, 3220.	2.9	17
40	Integrated multimodal photoacoustic microscopy with OCT- guided dynamic focusing. Biomedical Optics Express, 2019, 10, 137.	2.9	16
41	Single-Shot Dimension Measurements of the Mouse Eye Using SD-OCT. Ophthalmic Surgery Lasers and Imaging Retina, 2012, 43, 252-256.	0.7	14
42	Laser-scanning photoacoustic microscopy with ultrasonic phased array transducer. Biomedical Optics Express, 2012, 3, 2694.	2.9	13
43	Simultaneous optical coherence tomography and lipofuscin autofluorescence imaging of the retina with a single broadband light source at 480nm. Biomedical Optics Express, 2014, 5, 4242.	2.9	12
44	Regenerative potential of the zebrafish corneal endothelium. Experimental Eye Research, 2013, 106, 1-4.	2.6	10
45	Accommodation-induced variations in retinal thickness measured by spectral domain optical coherence tomography. Journal of Biomedical Optics, 2014, 19, 096012.	2.6	10
46	Measuring retinal blood flow in rats using Doppler optical coherence tomography without knowing eyeball axial length. Medical Physics, 2015, 42, 5356-5362.	3.0	9
47	Ultra-High Resolution Spectral Domain Optical Coherence Tomography of Traumatic Maculopathy. Ophthalmic Surgery Lasers and Imaging Retina, 2009, 40, 516-521.	0.7	9
48	Integrating photoacoustic microscopy, optical coherence tomography, OCT angiography, and fluorescence microscopy for multimodal imaging. Experimental Biology and Medicine, 2020, 245, 342-347.	2.4	8
49	Depth-resolved rhodopsin molecular contrast imaging for functional assessment of photoreceptors. Scientific Reports, 2015, 5, 13992.	3.3	7
50	Visible light OCT-based quantitative imaging of lipofuscin in the retinal pigment epithelium with standard reference targets. Biomedical Optics Express, 2018, 9, 3768.	2.9	6
51	Optical coherence photoacoustic microscopy (OC-PAM) with an intensity-modulated continuous-wave broadband light source. Journal of Optics (United Kingdom), 2016, 18, 064001.	2.2	5
52	Quantifying lipofuscin in retinal pigment epithelium in vivo by visible-light optical coherence tomography-based multimodal imaging. Scientific Reports, 2020, 10, 2942.	3.3	5
53	A2E Distribution in RPE Granules in Human Eyes. Molecules, 2020, 25, 1413.	3.8	5
54	Comparative study of optical coherence tomography angiography algorithms for rodent retinal imaging. Experimental Biology and Medicine, 2021, 246, 2207-2213.	2.4	5

SHULIANG JIAO

#	Article	IF	CITATIONS
55	Optical coherence tomography-guided dynamic focusing for combined optical and mechanical scanning multimodal photoacoustic microscopy. Journal of Biomedical Optics, 2019, 24, 1.	2.6	5
56	In vivo imaging rhodopsin distribution in the photoreceptors with nano-second pulsed scanning laser ophthalmoscopy. Quantitative Imaging in Medicine and Surgery, 2015, 5, 63-8.	2.0	5
57	Reply to Comment on "Optical-fiber-based Mueller optical coherence tomography― Optics Letters, 2004, 29, 2875.	3.3	4
58	Visible-light optical coherence tomography-based multimodal system for quantitative fundus autofluorescence imaging. Experimental Biology and Medicine, 2018, 243, 1265-1274.	2.4	4
59	Integrating photoacoustic microscopy with other imaging technologies for multimodal imaging. Experimental Biology and Medicine, 2021, 246, 771-777.	2.4	4
60	Biomedical optical imaging technology and applications: From basic research toward clinical diagnosis. Experimental Biology and Medicine, 2020, 245, 269-272.	2.4	3
61	DC Discharge Enhancement of Chemical Activity in Laser-Produced Plasma. Japanese Journal of Applied Physics, 1994, 33, 1018-1022.	1.5	2
62	PRELIMINARY STUDY ON SKIN CANCER DETECTION IN SENCAR MICE USING MUELLER OPTICAL COHERENCE TOMOGRAPHY. Journal of Innovative Optical Health Sciences, 2009, 02, 289-294.	1.0	2
63	Multiple-channel Mueller-matrix optical coherence tomography in biological tissue. , 0, , .		1
64	Polarization in low coherence interferometry. , 2009, 2009, 110-3.		0
65	Emerging imaging developments in experimental vision sciences and ophthalmology. Experimental Biology and Medicine, 2021, 246, 2137-2139.	2.4	0